THE JOURNAL OF PHYSICAL CHEMISTRY C
A JOURNAL OF THE AMERICAN CHEMICAL SOCIETY

pubs.acs.org/JPCC

Article

Prediction of Stable Silver Fluorides

Nikita Rybin,* Ilya Chepkasov, Dmitry Y. Novoselov, Vladimir I. Anisimov, and Artem R. Oganov*

Cite This: J. Phys. Chem. C 2022, 126, 15057−15063

Read Online

ACCESS | Metrics & More | Article Recommendations | Supporting Information

ABSTRACT: Silver fluorides form a variety of stable compounds at ambient and high-pressure conditions, but existing experiments and theoretical predictions provide an incomplete picture. Using a first-principles variable-composition evolutionary algorithm, we searched for stable silver fluorides at pressures up to 300 GPa. The obtained pressure−composition phase diagram is rather different from previous theoretical results and contains hitherto unknown phases. We discuss the predicted phases and provide a detailed description of the electronic correlation effects in the Ag−F system.

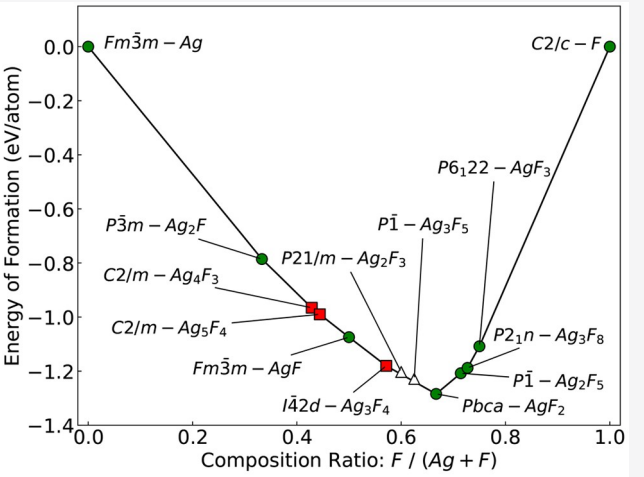

INTRODUCTION

The study of transition metal fluorides is a mature research field.[1,2] Transition metals easily adopt high oxidation states in fluorides[3] because of the extreme electronegativity of F. This trend is enhanced at high pressures—it is well-known that pressure can profoundly affect the chemical properties of the elements, leading to formation of unusual stoichiometries.[4,5]

Recently, fluorides of copper (Cu), silver (Ag), and gold (Au) have attracted considerable attention. From the fundamental point of view, novel compounds in the Cu−F and Ag−F systems exhibit curious magnetic properties.[6−8] AgF_2 is considered as a potential prototype of a new family of high-temperature superconductors,[9−15] whereas it was predicted that compression leads to the formation of gold fluorides with unusually high (+4 and +6) oxidation states of Au.[16] From the application standpoint, known Cu and Ag fluorides are already utilized in electrochemistry.[17−21]

Crystal structure prediction has been fruitfully applied to noble metal fluorides[6,16,22] and other transition metal fluorides,[23,24] especially at high-pressure conditions. In an old-style approach, crystal structure prediction was done for particular stoichiometries.[16,22−24] However, such fixed-composition search limits the prediction of new phases in the whole system. For example, the initial search for the Ag−F system was based on the fixed-stoichiometry methodology,[16] whereas the more recent analysis has led to the prediction of additional phases.[22] This was also a fixed-composition study,[22] and the results may still be incomplete. From our experience with the Cu−F[6] and many other systems,[25,26] we believe that the comprehensive analysis of the Ag−F system remains to be done. The system is interesting not only because of the rich chemical space[22] but also because of a possibility to find new high-temperature superconductors.[9,12,27,28] The experimental works dedicated to the Ag−F system under high pressures are rare;[12,29] combined experimental−theoretical works could facilitate new findings.

In this research, we present a first-principle variable-composition evolutionary crystal structure prediction study of the Ag−F system. The calculations were done for pressures from ambient up to 300 GPa. We recovered the experimentally known phases and report hitherto unknown stable phases, with the description of their structural features and electronic properties. As we shall see, pressure stabilizes a variety of novel compounds. The main focus of this work is the exploration of the chemical space of the Ag−F system and description of the general trends brought by compression.

METHODS

Stable phases in the Ag−F system were predicted using the first-principles evolutionary algorithm implemented in the

Received: July 7, 2022
Revised: August 11, 2022
Accepted: August 16, 2022
Published: August 30, 2022

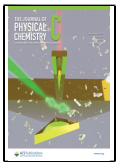

USPEX package.[30−32] The evolutionary search was combined with structure relaxations and energy calculations using the density functional theory (DFT) within the Perdew−Burke−Ernzerhof (PBE)[33] exchange−correlation functional and employing the projector augmented wave (PAW) method[34] as implemented in the VASP package.[35] During the variable-composition structure search, the first generation of 160 structures was produced using random symmetric[32] and random topological[36] structure generators, with up to 18 atoms in the primitive cell. To obtain 70% of the next generation (each subsequent generation contains 100 structures), variation operators (heredity, softmutation, transmutation, and lattice mutation) were applied to the 70% of the lowest-energy structures of the current generation, and the other 30% of the next generation were produced randomly. The percentage of structures produced by each of the variation operators was dynamically adjusted on-the-fly, based on the performance of each operator.[36] During the structure search, each generation of structures was relaxed through a series of steps with increasing precision. In the last step, we did single-point calculations using a plane-wave energy cutoff of 650 eV and Γ-centered *k*-meshes with a reciprocal space resolution of $2\pi \times 0.05$ Å^{-1} for Brillouin zone sampling, ensuring the convergence of the total energy evaluation.

The cornerstone of the variable-composition structure prediction is the convex hull construction, which determines the stability of compounds at particular thermodynamic conditions. Phases located on the convex hull are stable with respect to decomposition into elemental Ag and F or other Ag−F compounds. The convex hull is constructed geometrically on a diagram of the enthalpy of formation versus composition. The enthalpy of formation is defined as

$$\Delta H(\mathrm{Ag}_x\mathrm{F}_y) = (H(\mathrm{Ag}_x\mathrm{F}_y) - xH(\mathrm{Ag}) - yH(\mathrm{F}_2)/2) /(x + y) \quad (1)$$

The convex hull diagram of the Ag−F system obtained here (Figure 1) was constructed using the spin-polarized DFT calculations with SCAN exchange correlation functional.[37] It has been shown that SCAN improves the description of the energy of formation,[38] which has been emphasized for the Ag−F system.[22] In our calculations, we also observed that SCAN leads to the stabilization of the experimentally known low-pressure $Fm\bar{3}m$-AgF phase,[39] which is above the convex hull by 0.017 eV/atom when calculated using the PBE functional. The comparison of the convex hulls obtained using the PBE and SCAN is presented in the Supporting Information, Figure S1.

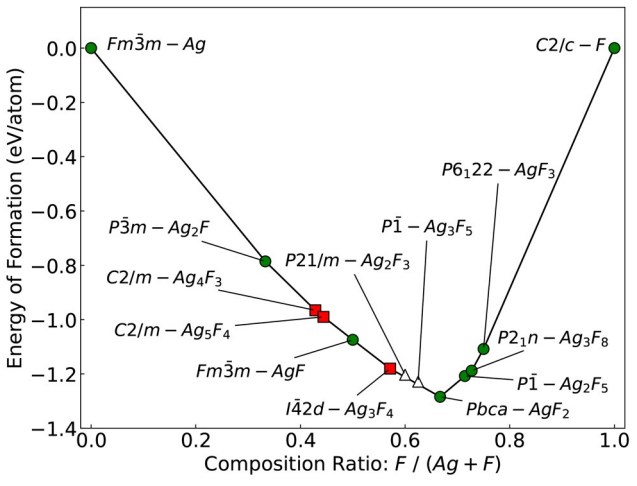

Figure 1. Convex hull of the Ag−F system at zero pressure, constructed on the basis of eq 1 and the spin-polarized DFT calculations with the SCAN exchange−correlation functional. Green circles represent experimentally known structures, red squares, theoretically predicted stable structures, and white triangles, experimentally unknown, slightly metastable structures.

The dynamical stability of all novel structures was verified with phonon calculations using the supercell approach and the finite displacement method,[40] as implemented in the Phonopy package.[41] The phonon dispersion curves were plotted using Sumo software.[42] The absence of imaginary frequencies indicates the dynamical stability of the predicted compounds.

The outer 4d electron shell of Ag ions can be filled partially, which indicates the importance of considering the Coulomb interaction between the electrons in these states. Silver ions in the oxidation state +1 have a completely filled 4d shell and are nonmagnetic, whereas ions in the oxidation state +2 are magnetic because they have one unpaired electron. Also, a strong Jahn−Teller effect can be expected for silver ions with $4d^9$ shell. Ions in the oxidation state +3 can be in two possible spin states−low-spin and high-spin, exhibiting nonmagnetic and magnetic properties, respectively. In addition, mixed-valence states with fractional oxidation states are also possible−they are characterized by the presence of a narrow or zero energy gap. Some of the considered compounds can be assigned to the class of strongly correlated systems. The Coulomb interaction between the electrons of the outer partially filled shell of a silver atom in these materials leads to several phenomena characteristic of correlated materials such as the metal−insulator transition due to a bandgap opening, local and band magnetism with the formation of a long-range magnetic order, and the Jahn−Teller effect. To study the properties related to the electronic correlation effects, we took into account the Coulomb interactions using the DFT+U approach.[43]

RESULTS AND DISCUSSION

The obtained convex hull contains experimentally known $Pm\bar{3}m$-AgF, *Pbca*-AgF_2, $P\bar{3}m$-Ag_2F, $P2_1n$-Ag_3F_8, $P\bar{1}$-Ag_2F_5, and $P6_122$-AgF_3,[44] which indicates the reliability of the chosen methods. Using the DFT−D3 approach,[45] we also checked that the van der Waals correction does not affect the convex hull diagram, which is consistent with the previous studies.[22,23] As has been shown,[46] the PBE functional makes it possible to correctly predict the ground state phase of fluorine—*C*2/*c*-F (*α*-F), which had been determined experimentally.[47,48] The high-pressure phase *Cmca*-F, which has been predicted earlier,[49] was also found in our calculations and was used for calculating the enthalpy of formation at high pressures in this work and in previous reports.[16,22]

To explore the Ag−F chemical space under pressure, we performed a crystal structure search at 50, 100, and 300 GPa (Supporting Information, Figures S2a,b and S3). The variable-composition crystal structure prediction calculations at 300 GPa revealed that AgF_4 is the silver fluoride with the highest fraction of F atoms, which adopts *C*2/*m* space group at 300 GPa, consistent with the previous study.[16] However, observing no significant differences between the results obtained at 100 and 300 GPa, we computed the pressure−phase diagram only up to 100 GPa. In particular, we tightly relaxed the compounds

https://doi.org/10.1021/acs.jpcc.2c04785
J. Phys. Chem. C 2022, 126, 15057−15063

predicted at 0, 50, and 100 GPa (metastable compounds up to 20 meV/atom were also taken into account) going from 0 to 100 GPa with a step of 20 GPa. These calculations allowed us to construct the pressure−composition phase diagram presented in Figure 2.

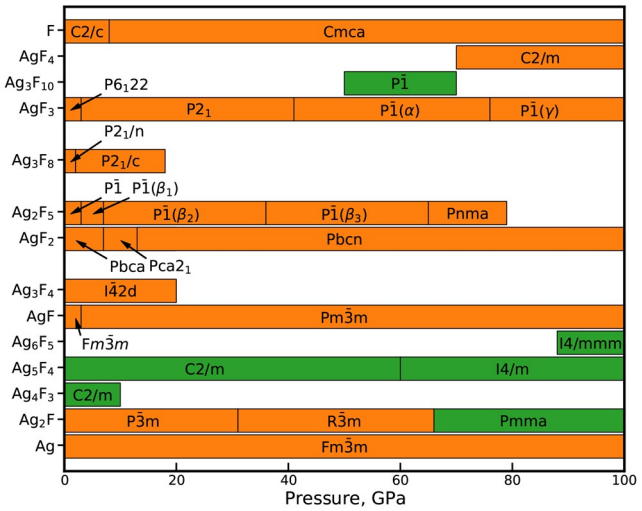

Figure 2. Calculated pressure−composition phase diagram of the Ag−F system. Novel phases (*Pmma*-Ag_2F, *C*2/*m*-Ag_4F_3, *C*2/*m*-Ag_5F_4, *I*4/*m*-Ag_5F_4, *I*4/*mmm*-Ag_6F_5, and $P\bar{1}$-Ag_3F_{10}) are highlighted in green.

Known Ag−F compounds (AgF, AgF_2, AgF_3) have silver in the oxidation states +1, + 2, and +3, respectively. Consequently, compounds with the Ag/F ratio above 1 should contain silver in a formal oxidation state lower than +1. This is the case of known silver subfluoride Ag_2F (oxidation state $+^1/_2$),[50] which at ambient conditions adopts the anti-CdI_2 structure ($P\bar{3}m$).[51] It has been predicted in the previous study[22] that at 39 GPa, the anti-CdI_2 structure transforms into anti-$CdCl_2$ (space group $R\bar{3}m$). Then at 65 GPa, another transition from $R\bar{3}m$-Ag_2F into the tetragonal structure with space group *I*4/*mmm* occurs, and finally, from 91 GPa, the lowest enthalpy Ag_2F adopts space group *P*4/*mmm*. Our results for Ag_2F are different: we found another phase transition from the anti-$CdCl_2$ structure ($R\bar{3}m$-Ag_2F) to *Pmma*-Ag_2F (Figure 3a), which takes place at approximately 65 GPa (Figure 4). The enthalpy of formation of *Pmma*-Ag_2F

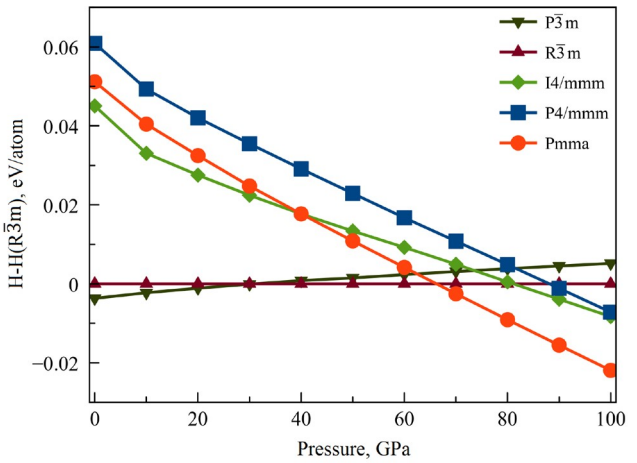

Figure 4. Enthalpy of various Ag_2F phases relative to the $R\bar{3}m$ phase.

is lower than that of the earlier predicted phases *I*4/*mmm* and *P*4/*mmm* by 7.5 meV/atom at 70 GPa and by 13.6 meV/atom at 100 GPa.[22] The phonon spectrum of *Pmma*-Ag_2F computed at 100 GPa does not have imaginary frequencies (Supporting

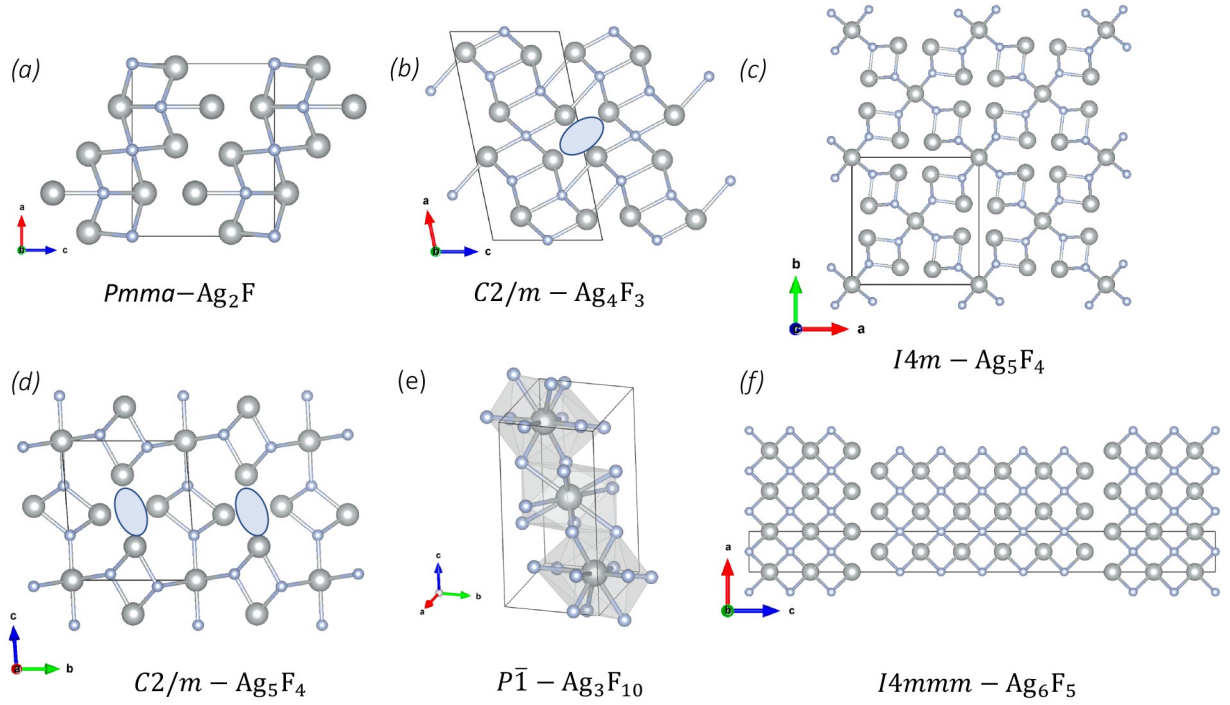

Figure 3. Schematic representation of the predicted crystal structures. The Ag and F atoms are shown in gray and light purple, respectively. The structures were visualized using VESTA.[52]

https://doi.org/10.1021/acs.jpcc.2c04785
J. Phys. Chem. C 2022, 126, 15057−15063

Information, Figure S4g) . *Pmma*-Ag_2F has a layered structure containing seven-coordinated fluorine-centered polyhedrons FAg_7. Three nonequivalent Ag atoms have different surroundings: in the first site, the Ag atom is coordinated with six F atoms; in the second site, Ag is bound to four F atoms; and the third nonequivalent Ag atom is bound to the surrounding Ag atoms and to only one F atom.

At zero pressure and temperature, we found two hitherto unknown thermodynamically and dynamically stable nonmagnetic structures $C2/m$-Ag_4F_3 and $C2/m$-Ag_5F_4 (Figure 1 and Supporting Information, Figure S4a,b). These compounds have Ag in the oxidation state lower than 1. At zero pressure, ground-state Ag_4F_3 and Ag_5F_4 crystallize in the monoclinic space group $C2/m$ (Figure 3b,d). Although the structures are not exactly homologous, they contain similar features: distorted Ag_6F octahedrons and columns of empty Ag_6 octahedrons (indicated by ellipses in Figure 3b,d). If these compounds were electrides, electrons could be localized in these cages. However, the electron localization function that we computed makes us conclude that these materials are not electrides. We also found that Ag_5F_4 has a pressure-induced phase transition at 50 GPa and crystallizes above that pressure in the tetragonal space group $I4/m$ (Figure 3c). In the $I4/m$-Ag_5F_4 crystal, the F atom is bound to five Ag atoms to form edge- and corner-sharing distorted Ag_5F trigonal bipyramids.

Compounds between AgF and AgF_2 have silver in the mixed-valence state +1 and +2, whereas in compounds between AgF_2 and AgF_3, the mixed-valence state of Ag is 2+ and 3+. The latter region contains well-known Ag_2F_5 and Ag_3F_8. Ag^{2+} ions have $4d^9$ outer electron shell configuration with one unpaired electron. Such systems can exhibit magnetic properties as well as correlation effects. To study these properties, we performed calculations using the DFT and DFT+U methods with spin polarization at zero pressure. Electronic correlations and spin polarization were taken into account by the rotationally invariant DFT+U method,[53] in which we used the Coulomb interaction parameter U = 5 eV and the exchange interaction parameter J = 0.65 eV reported in the earlier study of the magnetic coupling constants in silver difluoride.[54] The density of states of the investigated silver fluorides calculated using the DFT and DFT+U methods is shown in the Supporting Information, Figures S7−S13. The resulting values of the total energy and magnetic moment are presented in theSupporting Information, Tables S4 and S5, the distribution of magnetic moments for AFM solutions are shown in Figure S14. Taking into account the correlation effects and magnetism did not change the relative position of the considered systems on the convex hull diagram at zero pressure.

The DFT+U calculations show that Ag_4F_3 is nonmagnetic. Despite the fact that Ag_5F_4 has a mixed valence and its formal valence formula contains $4d^9$ silver ions, it is also nonmagnetic. The Ag_2F system relaxes to nonmagnetic state regardless of the starting magnetic ordering. Therefore, the total energies listed in the Supporting Information, Table S4, are the same. Ag_2F_5 is a metal with a mixed Ag^{2+}/Ag^{3+} valence. The total energies for different types of magnetic ordering of Ag_2F_5 are also very close because the magnetic ions have a similar magnitude of the moment and alternate diamagnetic ones with a negligible magnetic moment. In the DFT+U, the magnetic moments of Ag^{2+} ions are about 0.5 μ_B, whereas Ag^{3+} ions are nonmagnetic. In both DFT and DFT+U, Ag_2F_5 is a metal.

The novel phase $I\bar{4}2d$-Ag_3F_4 has been predicted[22] in the region between AgF and AgF_2. This structure is metallic in both the DFT and DFT+U and has a magnetic solution in the DFT with small magnetic moments of 0.04−0.09 μ_B. Ag_3F_4 has a mixed Ag^{1+}/Ag^{2+} valence, but in the DFT+U both types of the Ag ions have the same magnetic moments of 0.2 μ_B. Further comparing our results with those previously published,[16,22] we note that both $P\bar{1}$-Ag_3F_5 and $P2_1/m$-Ag_2F_3 are predicted here to be slightly metastable by 1 meV/atom (Figure 1). $P2_1/m$-Ag_2F_3 found in our search has been predicted[22] as "marginally stable" at ambient pressure. The most stable structure of Ag_3F_5 found in our study is low-symmetry $P\bar{1}$-Ag_3F_5. We stress that $P2_1/m$-Ag_2F_3 has phonons with imaginary frequencies, whereas $P\bar{1}$-Ag_3F_5 predicted here has a phonon spectrum without imaginary frequencies (Figure S4c,d). Ag_3F_5 also has a mixed Ag^{1+}/Ag^{2+} valence with magnetic moments equal to 0.6 and 0.3 μ_B. Ag_3F_5 is a metal in the DFT but insulator with a small energy gap of about 0.2 eV in the DFT+U.

In *Pbca*-AgF_2, there are only 2+ valence silver ions with a magnetic moment of 0.6 μ_B. It is a metal in the DFT and an insulator in the DFT+U with an energy gap of about 1.2 eV between the 2p-F and 4d-Ag states. The considered magnetic configurations have a tiny effect on the total energy (≈0.01 eV/atom), which may indicate significant spin fluctuations and support the idea of silver-fluoride-based analogs of cuprate superconductors.[12] Silver ions with a valence of 2+ have one unpaired electron in the 4d shell and thus can be Jahn−Teller-active ions in an octahedral coordination. For example, in AgF_2, the $4d^9$ ions are located in an octahedral environment and contain a nondegenerate e_g subshell, which is accompanied by octahedron elongation characteristic of the Jahn−Teller effect (2 × 2.218, 2 × 2.196, and 2 × 2.574 Å).

Perhaps the most interesting compound is AgF_4 because of the intriguing possibility of the unusual Ag(IV) valence state. The results of the previous studies of the compound show some disagreement. Kurzydlowski et al.[22] have predicted that $C2/m$-AgF_4 is stable from 56 to 69 GPa and transforms to $I4/m$-AgF_4 above that pressure, whereas the other research group has shown that $I4/m$-AgF_4 dominates in the region from 50 to 200 GPa.[16] In our calculations, we found that the $C2/m$ phase has the lowest enthalpy from approximately 70 GPa to at least 100 GPa (the maximum pressure used for constructing the pressure−phase diagram), although the energy difference between $C2/m$ and $I4/m$ phases is very small (0.6−0.7 meV/atom). In the pressure range from 20 to 50 GPa, $I4/m$-AgF_4 has the lowest enthalpy but is still above the convex hull.

Recently, we have explored the emergence of anomalously high valence states under pressure,[55] and now can estimate electronegativities of the relevant atoms and ions on the basis of that work. Whereas at 50 GPa the electronegativity of Ag^{4+} (11.7 eV) is much higher than that of F (5.6 eV) and F^- (−2.6 eV), which implies the back transfer of the charge to Ag^{4+}, the situation changes at higher pressures. At 200 GPa, the electronegativity of Ag^{4+} (5.4 eV) is similar to that of F (5.2 eV). At 500 GPa, the electronegativity of Ag^{4+} (0.7 eV) is much lower than that of F (5.1 eV) and comparable to that of F^- (−0.2 eV), indicating that proper Ag^{4+} is likely at 500 GPa but problematic at 50 GPa.

Using the density matrix to determine the occupation numbers, we found that the valence of silver in Ag−F compounds can be +1 (Ag_2F), + 2 (AgF_2), and +3 (AgF_3), as well as have a mixed character (Ag_3F_4, Ag_2F_5). The valence 4+ expected in AgF_4 is not observed because this compound is a metal and an electron hole is formed in the metallic band,

https://doi.org/10.1021/acs.jpcc.2c04785
J. Phys. Chem. C 2022, 126, 15057−15063

which is a superposition of the p states of the ligands and the d states of the metal ions, but not in the 4d-Ag shell by analogy with doped cuprates. Therefore, silver in AgF_4 has an atomic configuration $4d^8$ and valence (III), not $4d^7$ (IV). In this case, the magnetism is not localized but band-type, with a small magnetic moment of 0.12 μ_B, unlike, for example, AgF_2, where silver has $4d^9$ (II) configuration and exhibits a moment of 0.64 μ_B.

Ag−F compounds containing silver with an integer valence are nonmetals. In systems with the Ag^{2+} and Ag^{3+} ions, the energy gap has a width of about 1.2 and 0.9 eV, respectively, whereas the Ag^{2+} ($4d^9$) ions have local magnetic moments, and the Ag^{3+} ($4d^8$) ions are in a low-spin state with $S = 0$. The $Fm\bar{3}m$-AgF system with Ag^{1+} ions, with a completely filled 4d shell, demonstrates a zero-energy gap and the absence of a magnetic moment. Compounds with a fractional mixed valence lower than +1 are nonmagnetic poor metals with a low density of states near the Fermi level, whereas compounds with an intermediate valence between +1 and +3 are magnetic (between $4d^{10}$ and $4d^8$). $I\bar{4}2d$-Ag_3F_4 and $P\bar{1}$-Ag_2F_5 are ferromagnetic metals, whereas $P\bar{1}$-Ag_3F_5 and Ag_3F_8 are antiferromagnetic insulators with E_{gap} = 0.2 and 1 eV, respectively. Thus, compounds in which the valence of silver is strictly higher than +1 but lower than or equal to +3 clearly demonstrate the characteristic features of systems with strong electronic correlations. Application of an external pressure to such systems will lead to broadening of the 4d bands of silver—which will contribute to the decrease in the localization of the magnetic moments—and to emergence of the density of states at the Fermi level.

A surprising number of stable and low-enthalpy metastable phases were observed in the entire pressure range (see the convex hulls constructed at 50 and 100 GPa in Supporting Information, Figure S2). Many of these phases are structurally similar (Supporting Information, Figure S5) and can intergrow or form defective regions with each other, or both. Non-stoichiometric phases can also be expected. Notably, although many metastable compounds are slightly above the convex hull, they have phonon spectra without imaginary frequencies (Supporting Information, Figure S6). Among all compounds obtained at high pressures, we discovered several unexpected stable structures, such as $P\bar{1}$-Ag_3F_{10} (stable from approximately 50 to 70 GPa) and $I4/mmm$-Ag_6F_5 (stable from 90 GPa). The structures are dynamically stable (Supporting Information, Figure S4f,h). Ag_3F_{10} and Ag_6F_5 crystallize in the triclinic group $P\bar{1}$ and the tetragonal $I4/mmm$ phase, respectively (Figure 3e,f).

CONCLUSION

We investigated the pressure−composition phase diagram of the Ag−F system. The results of the systematic crystal structure search revealed six hitherto unknown stable phases. The calculations show that silver fluorides have rich polymorphism both at ambient conditions and under pressure. We showed that an extensive prediction of stable compounds should be done using a variable-composition stoichiometry search. Besides, considering the Coulomb interactions between the localized electronic states of transition metal ions makes it possible to reveal a rich set of properties associated with the correlation effects, including the metal−insulator transition, band-type, and localized magnetism, as well as the Jahn−Teller effect.

ASSOCIATED CONTENT

Supporting Information

Supporting Information contains the structural data, phonon spectra, and DFT+U calculation data for all new compounds. The Supporting Information is available free of charge at https://pubs.acs.org/doi/10.1021/acs.jpcc.2c04785.

(PDF)

AUTHOR INFORMATION

Corresponding Authors

Nikita Rybin − *Skolkovo Institute of Science and Technology, Moscow 121205, Russia;* orcid.org/0000-0001-7053-5295; Email: nikita.rybin@skoltech.ru

Artem R. Oganov − *Skolkovo Institute of Science and Technology, Moscow 121205, Russia;* orcid.org/0000-0001-7082-9728; Email: artem.oganov@skoltech.ru

Authors

Ilya Chepkasov − *Skolkovo Institute of Science and Technology, Moscow 121205, Russia;* orcid.org/0000-0001-8376-2999

Dmitry Y. Novoselov − *Skolkovo Institute of Science and Technology, Moscow 121205, Russia; Department of Theoretical Physics and Applied Mathematics, Ural Federal University, Yekaterinburg 620002, Russia; M. N. Mikheev Institute of Metal Physics of Ural Branch of Russian Academy of Sciences, Yekaterinburg 620137, Russia;* orcid.org/0000-0003-1668-3734

Vladimir I. Anisimov − *Skolkovo Institute of Science and Technology, Moscow 121205, Russia; Department of Theoretical Physics and Applied Mathematics, Ural Federal University, Yekaterinburg 620002, Russia; M. N. Mikheev Institute of Metal Physics of Ural Branch of Russian Academy of Sciences, Yekaterinburg 620137, Russia*

Complete contact information is available at: https://pubs.acs.org/10.1021/acs.jpcc.2c04785

Notes

The authors declare no competing financial interest.

ACKNOWLEDGMENTS

This work was supported by the Russian Science Foundation (Project 19-72-30043). The calculations were performed using Arkuda and Oleg supercomputers of Skoltech.

REFERENCES

(1) Winfield, J. M. Transition metal fluorides. *J. Fluorine Chem.* **1986**, *33*, 159−178.

(2) Thrasher, J. S.; Strauss, S. H. *Inorganic Fluorine Chemistry*; 1994; Chapter 1, pp 1−23.

(3) Higelin, A.; Riedel, S. In *Modern Synthesis Processes and Reactivity of Fluorinated Compounds*; Groult, H., Leroux, F. R., Tressaud, A., Eds.; Elsevier: 2017; pp 561−586.

(4) Zhang, L.; Wang, Y.; Lv, J.; Ma, Y. Materials discovery at high pressures. *Nat. Rev. Mater.* **2017**, *2*, 1−16.

(5) Miao, M.; Sun, Y.; Zurek, E.; Lin, H. Chemistry under high pressure. *Nature Reviews Chemistry* **2020**, *4*, 508−527.

(6) Rybin, N.; Novoselov, D. Y.; Korotin, D. M.; Anisimov, V. I.; Oganov, A. R. Novel copper fluoride analogs of cuprates. *Phys. Chem. Chem. Phys.* **2021**, *23*, 15989−15993.

(7) Korotin, D. M.; Novoselov, D. Y.; Anisimov, V. I.; Oganov, A. R. Mixed spin S= 1 and S= 1/2 layered lattice in Cu_2F_5. *Phys. Rev. B* **2021**, *104*, 064410.

(8) Xu, X.; Ma, Y.; Zhang, T.; Lei, C.; Huang, B.; Dai, Y. Prediction of two-dimensional antiferromagnetic ferroelasticity in an AgF2 monolayer. *Nanoscale Horiz.* **2020**, *5*, 1386−1393.
(9) Grochala, W.; Hoffmann, R. Real and Hypothetical Intermediate-Valence Ag^{II}/Ag^{III} and Ag^{II}/Ag^{I} Fluoride Systems as Potential Superconductors. *Angew. Chem., Int. Ed.* **2001**, *40*, 2742−2781.
(10) Kurzydłowski, D. The jahn-teller distortion at high pressure: The case of copper difluoride. *Crystals* **2018**, *8*, 140.
(11) Kurzydłowski, D.; Derzsi, M.; Barone, P.; Grzelak, A.; Struzhkin, V.; Lorenzana, J.; Grochala, W. Dramatic enhancement of spin-spin coupling and quenching of magnetic dimensionality in compressed silver difluoride. *Chem. Commun.* **2018**, *54*, 10252−10255.
(12) Gawraczynski, J.; et al. Silver route to cuprate analogs. *Proc. Natl. Acad. Sci. U.S.A.* **2019**, *116*, 1495−1500.
(13) Kurzydłowski, D.; Grochala, W. Prediction of Extremely Strong Antiferromagnetic Superexchange in Silver(II) Fluorides: Challenging the Oxocuprates(II). *Angew. Chem.* **2017**, *129*, 10248−10251.
(14) Grzelak, A.; Su, H.; Yang, X.; Kurzydłowski, D.; Lorenzana, J.; Grochala, W. Epitaxial engineering of flat silver fluoride cuprate analogs. *Phys. Rev. Mater.* **2020**, *4*, 084405.
(15) Bandaru, S.; Derzsi, M.; Grzelak, A.; Lorenzana, J.; Grochala, W. Fate of doped carriers in silver fluoride cuprate analogs. *Phys. Rev. Mater.* **2021**, *5*, 064801.
(16) Lin, J.; Zhang, S.; Guan, W.; Yang, G.; Ma, Y. Gold with + 4 and + 6 Oxidation States in AuF4 and AuF6. *J. Am. Chem. Soc.* **2018**, *140*, 9545−9550.
(17) Wang, F.; et al. Conversion reaction mechanisms in lithium ion batteries: Study of the binary metal fluoride electrodes. *J. Am. Chem. Soc.* **2011**, *133*, 18828−18836.
(18) Wang, F.; Yu, H. C.; Chen, M. H.; Wu, L.; Pereira, N.; Thornton, K.; Van Der Ven, A.; Zhu, Y.; Amatucci, G. G.; Graetz, J. Tracking lithium transport and electrochemical reactions in nanoparticles. *Nat. Commun.* **2012**, *3*, 1−8.
(19) Hua, X.; Robert, R.; Du, L.-S.; Wiaderek, K. M.; Leskes, M.; Chapman, K. W.; Chupas, P. J.; Grey, C. P. Comprehensive Study of the CuF_2 Conversion Reaction Mechanism in a Lithium Ion Battery. *J. Phys. Chem. C* **2014**, *118*, 15169−15184.
(20) Omenya, F.; Zagarella, N. J.; Rana, J.; Zhang, H.; Siu, C.; Zhou, H.; Wen, B.; Chernova, N. A.; Piper, L. F. J.; Zhou, G.; Whittingham, M. S. Intrinsic Challenges to the Electrochemical Reversibility of the High Energy Density Copper(II) Fluoride Cathode Material. *ACS Appl. Energy Mater.* **2019**, *2*, 5243−5253.
(21) Tong, W.; Amatucci, G. G. Silver copper fluoride: A novel perovskite cathode for lithium batteries. *J. Power Sources* **2017**, *362*, 86−91.
(22) Kurzydłowski, D.; Derzsi, M.; Zurek, E.; Grochala, W. Fluorides of silver under large compression. *Chemistry A European Journal* **2021**, *27*, 5536−5545.
(23) Lin, J.; Zhao, Z.; Liu, C.; Zhang, J.; Du, X.; Yang, G.; Ma, Y. IrF_8 Molecular Crystal under High Pressure. *J. Am. Chem. Soc.* **2019**, *141*, 5409−5414.
(24) Lin, J.; Du, X.; Rahm, M.; Yu, H.; Xu, H.; Yang, G. Exploring the Limits of Transition-Metal Fluorination at High Pressures. *Angew. Chem., Int. Ed.* **2020**, *59*, 9155−9162.
(25) Oganov, A. R.; Pickard, C. J.; Zhu, Q.; Needs, R. J. Structure prediction drives materials discovery. *Nat. Rev. Mater.* **2019**, *4*, 331−348.
(26) Boeri, L.; et al. The 2021 Room-Temperature Superconductivity Roadmap. *J. Phys.: Condens. Matter* **2021**, *34*, 183002.
(27) Grochala, W. The theory-driven quest for a novel family of superconductors: fluorides. *J. Mater. Chem.* **2009**, *19*, 6949−6968.
(28) Grochala, W.; Hoffmann, R. Real and Hypothetical Intermediate-Valence AgII/AgIII and AgII/AgI Fluoride Systems as Potential Superconductors. *Angew. Chem., Int. Ed.* **2001**, *40*, 2742−2781.
(29) Grzelak, A.; Gawraczyński, J.; Jaroń, T.; Kurzydłowski, D.; Budzianowski, A.; Mazej, Z.; Leszczyński, P. J.; Prakapenka, V. B.; Derzsi, M.; Struzhkin, V. V.; Grochala, W. High-Pressure Behavior of Silver Fluorides up to 40 GPa. *Inorg. Chem.* **2017**, *56*, 14651−14661.
(30) Oganov, A. R.; Glass, C. W. Crystal structure prediction using ab initio evolutionary techniques: Principles and applications. *J. Chem. Phys.* **2006**, *124*, 244704.
(31) Oganov, A. R.; Lyakhov, A. O.; Valle, M. How Evolutionary Crystal Structure Prediction Works and Why. *Acc. Chem. Res.* **2011**, *44*, 227−237.
(32) Lyakhov, A. O.; Oganov, A. R.; Stokes, H. T.; Zhu, Q. New developments in evolutionary structure prediction algorithm USPEX. *Comput. Phys. Commun.* **2013**, *184*, 1172−1182.
(33) Perdew, J. P.; Burke, K.; Ernzerhof, M. Generalized Gradient Approximation Made Simple. *Phys. Rev. Lett.* **1996**, *77*, 3865−3868.
(34) Blöchl, P. E. Projector augmented-wave method. *Phys. Rev. B* **1994**, *50*, 17953−17979.
(35) Kresse, G.; Furthmüller, J. Efficient iterative schemes for ab initio total-energy calculations using a plane-wave basis set. *Phys. Rev. B* **1996**, *54*, 11169−11186.
(36) Bushlanov, P. V.; Blatov, V. A.; Oganov, A. R. Topology-based crystal structure generator. *Comput. Phys. Commun.* **2019**, *236*, 1−7.
(37) Sun, J.; Ruzsinszky, A.; Perdew, J. P. Strongly Constrained and Appropriately Normed Semilocal Density Functional. *Phys. Rev. Lett.* **2015**, *115*, 036402.
(38) Sun, J.; Remsing, R. C.; Zhang, Y.; Sun, Z.; Ruzsinszky, A.; Peng, H.; Yang, Z.; Paul, A.; Waghmare, U.; Wu, X.; Klein, M. L.; Perdew, J. P. Accurate first-principles structures and energies of diversely bonded systems from an efficient density functional. *Nat. Chem.* **2016**, *8*, 831−836.
(39) Hull, S.; Berastegui, P. High-pressure structural behaviour of silver(I) fluoride. *J. Phys.: Condens. Matter* **1998**, *10*, 7945−7955.
(40) Parlinski, K.; Li, Z. Q.; Kawazoe, Y. First-Principles Determination of the Soft Mode in Cubic ZrO_2. *Phys. Rev. Lett.* **1997**, *78*, 4063−4066.
(41) Togo, A.; Tanaka, I. First principles phonon calculations in materials science. *Scripta Materialia* **2015**, *108*, 1−5.
(42) Ganose, A. M.; Jackson, A. J.; Scanlon, D. O. sumo: Command-line tools for plotting and analysis of periodic ab initio calculations. *Journal of Open Source Software* **2018**, *3*, 717.
(43) Zaanen, J.; Sawatzky, G. A.; Allen, J. W. Band gaps and electronic structure of transition-metal compounds. *Phys. Rev. Lett.* **1985**, *55*, 418−421.
(44) Žemva, B.; Lutar, K.; Jesih, A.; Casteel, W. J.; Wilkinson, A. P.; Cox, D. E.; von Dreele, R. B.; Borrmann, H.; Bartlett, N. Silver Trifluoride: Preparation, Crystal Structure, Some Properties, and Comparison with AuF_3. *J. Am. Chem. Soc.* **1991**, *113*, 4192−4198.
(45) Grimme, S.; Antony, J.; Ehrlich, S.; Krieg, H. A consistent and accurate ab initio parametrization of density functional dispersion correction (DFT-D) for the 94 elements H-Pu. *J. Chem. Phys.* **2010**, *132*, 154104.
(46) Mattsson, S.; Paulus, B.; Redeker, F. A.; Beckers, H.; Riedel, S.; Müller, C. The Crystal Structure of α-F 2: Solving a 50 Year Old Puzzle Computationally. *Chem. Eur. J.* **2019**, *25*, 3318−3324.
(47) Meyer, L.; Barrett, C. S.; Greer, S. C. Crystal Structure of -Fluorine. *J. Chem. Phys.* **1968**, *49*, 1902−1907.
(48) Pauling, L.; Keaveny, I.; Robinson, A. B. The crystal structure of -fluorine. *J. Solid State Chem.* **1970**, *2*, 225−227.
(49) Lv, Q.; Jin, X.; Cui, T.; Zhuang, Q.; Li, Y.; Wang, Y.; Bao, K.; Meng, X. Crystal structures and electronic properties of solid fluorine under high pressure. *Chinese Physics B* **2017**, *26*, 076103.
(50) Kawamura, H.; Shirotani, I.; Hirooka, T.; Fujihira, M.; Maruyama, Y.; Inokuchi, H. Photoemission from silver subfluoride, Ag_2F. *Chem. Phys. Lett.* **1972**, *15*, 594−595.
(51) Williams, A. Neutron powder diffraction study of silver subfluoride. *J. Phys.: Condens. Matter* **1989**, *1*, 2569−2574.
(52) Momma, K.; Izumi, F. VESTA: a three-dimensional visualization system for electronic and structural analysis. *J. Appl. Crystallogr.* **2008**, *41*, 653−658.

https://doi.org/10.1021/acs.jpcc.2c04785
J. Phys. Chem. C 2022, 126, 15057−15063

(53) Liechtenstein, A. I.; Anisimov, V. I.; Zaanen, J. Density-functional theory and strong interactions: Orbital ordering in Mott-Hubbard insulators. *Phys. Rev. B* **1995**, *52*, R5467−R5470.
(54) Miller, C.; Botana, A. S. Cupratelike electronic and magnetic properties of layered transition-metal difluorides from first-principles calculations. *Phys. Rev. B* **2020**, *101*, 195116.
(55) Dong, X.; Oganov, A. R.; Cui, H.; Zhou, X.-F.; Wang, H.-T. Electronegativity and chemical hardness of elements under pressure. *Proc. Natl. Acad. Sci. U. S. A.* **2022**, *119*, 2117416119.

https://doi.org/10.1021/acs.jpcc.2c04785
J. Phys. Chem. C 2022, 126, 15057−15063